Proceedings of the Reactor Physics Asia 2015 (RPHA15) Conference
Jeju, Korea, Sept. 16-18, 2015

Modeling of Axial Fuel Expansion Phenomenon in the BFS Critical Facility

Sunghwan Yun* and Sang Ji Kim
Korea Atomic Energy Research Institute (KAERI)
989-111 Daedeok-daero, Yuseong-gu, Daejeon, Korea, 305-353
**Corresponding author: syun@kaeri.re.kr*

1. Introduction

The Prototype Gen-IV Sodium-cooled Fast Reactor (PGSFR), which is planned to get specific design approval by 2020, is a pool-type, metal-fueled, blanket-free 150 MWe fast reactor [1]. The PGSFR will be operated with low enriched U-Zr fuel at the first phase; thereafter, the fuel of the PGSFR will be gradually changed to U-TRU-Zr fuel.

The metal-fueled SFR such as the PGSFR is known to be inherently safe at unprotected events owing to the low operating fuel temperature and negative reactivity feedback mechanism of the axial fuel expansion and radial core expansion [2, 3]. Several important tests of the EBR-II reactor support these characteristics based on a measurement of the integral reactivity [4].

However, the results of a sensitivity analysis during an Unprotected Loss Of Flow (ULOF) accident showed that these inherent safety characteristics of a metal-fueled SFR are dependent on the uncertainties of separated reactivities and reactor design [5]. Hence, validation of the separated reactivities of the PGSFR is a requisite work for specific design approval.

A physics experiment for the axial fuel expansion reactivity measurements for a 100 MWe uranium core was performed in the Russian BFS critical facility in 2012 by inserting a ring disk. Since the Russian BFS facility is composed of experimental rods filled by cylindrical disks, the insertion of the ring disk showed the reproduced reactivities well compared to the axial expansion reactivities of the target core [6, 7].

Another physical experiment for the axial fuel expansion reactivity measurements for the PGSFR core is planned to be performed in the Russian BFS facility during 2015.

In this paper, experimental models of the axial expansion reactivity measurements for the PGSFR core are described. The similarity of axial expansion reactivities in between the experimental models and the PGSFR core are also discussed.

2. Establishment of Experimental Models

2.1 Reference critical model

Radial and axial layouts of the target PGSFR core are shown in Figs. 1 and 2. The target core was composed of 52 inner core fuel assemblies, 60 outer core fuel assemblies, 90 steel reflector assemblies, and 102 B_4C shield assemblies. In the target core, 16.9 w/o enriched U-Zr fuels were loaded in the inner core while 17.4 w/o enriched U-Zr fuels were loaded in the outer core to represent the End of Effective Cycle (EOEC) core.

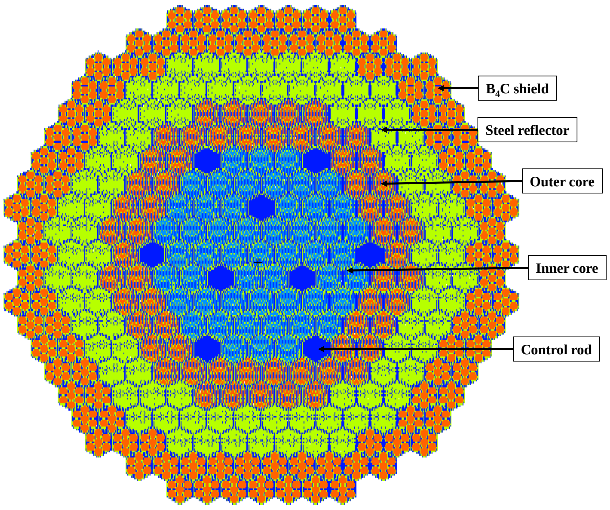

Fig. 1. Radial layout of the target PGSFR uranium core

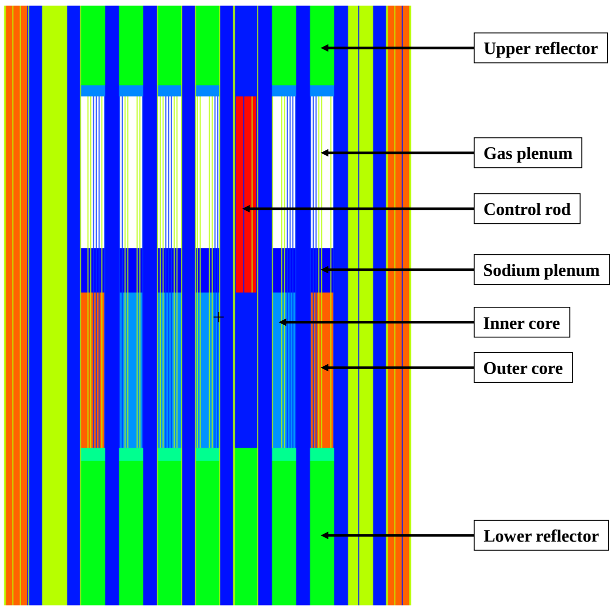

Fig. 2. Axial layout of the target PGSFR uranium core

The mock-up experimental model was made to conserve the mass and size of each region in the target core [8] (Semenov Mikhail, personal communication, April 22, 2015). Radial and axial layouts of the mock-up experimental models are shown in Figs. 3 and 4. Since the enrichment of two core regions in the target core differ, two different fuel unit cells were used, as shown in Fig. 5. Nine fuel unit cells were loaded in the inner core region and six fuel unit cells were loaded in the outer core region. Detailed information of each disk is listed in reference [9].

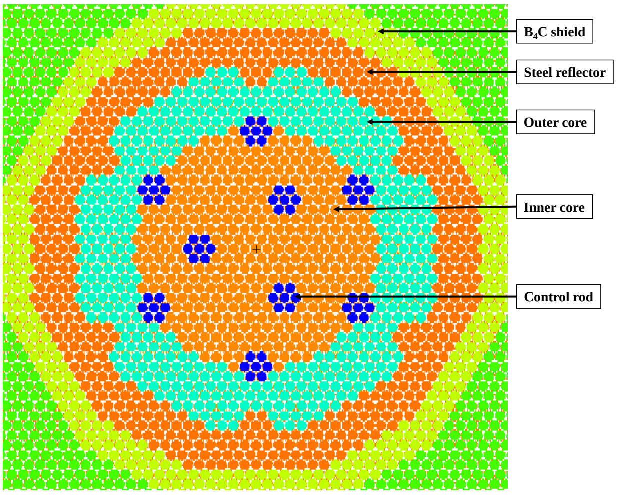

Fig. 3. Radial layout of the mock-up experimental model

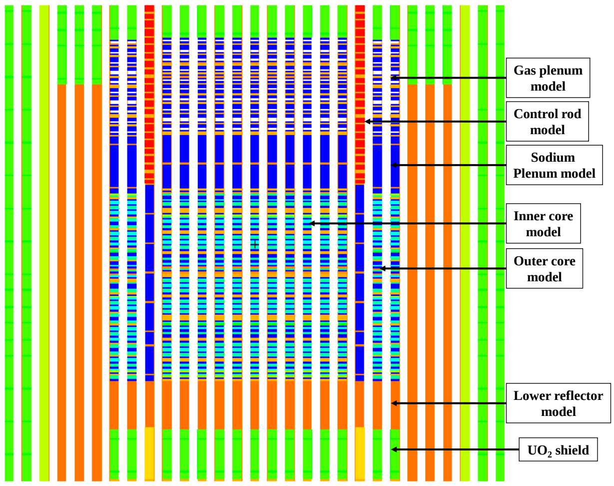

Fig. 4. Axial layout of the mock-up experimental model

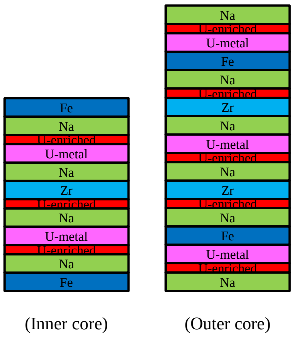

Fig. 5. Fuel unit cells of the mock-up experimental model

Although the mass and size were conserved in experimental model, there were significant differences in temperature; the mock-up experimental model was at room temperature whereas the target core was at the operating temperature. Since the mock-up model should reflect similar neutronic characteristics comparing to the target core at operating temperature instead of room temperature, some options were considered to compensate Doppler broadening effect and they were described at the reference [8].

Finally, to compensate for the Doppler broadening effect, enrichments of the fuel unit cell were designed slightly lower than those of the target core: 15.9 w/o for inner core and 16.8 w/o for outer core.

2.2 Axial Expansion Models

In the axial expansion models, three expansion cases were considered for each region to validate the axial fuel expansion reactivity coefficients. Although the fuels of the target core will be expanded up to 1 ~ 1.5 % in most of unprotected events, 2.5 ~ 9 % the expansion cases were selected due to the large size of the fuel unit cells. Axial expansion models for the inner and outer core fuels are shown in Figs. 6 and 7, respectively.

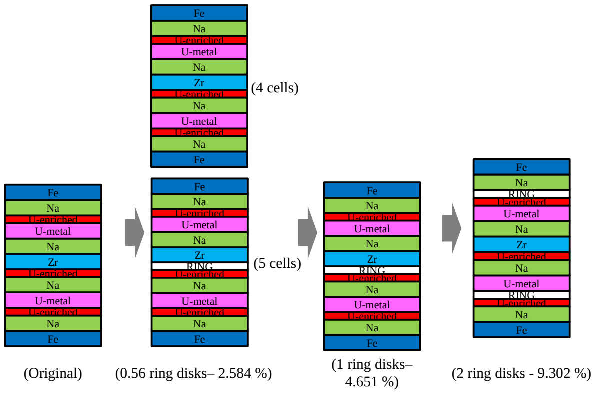

Fig. 6. Axial expansion models in the inner core

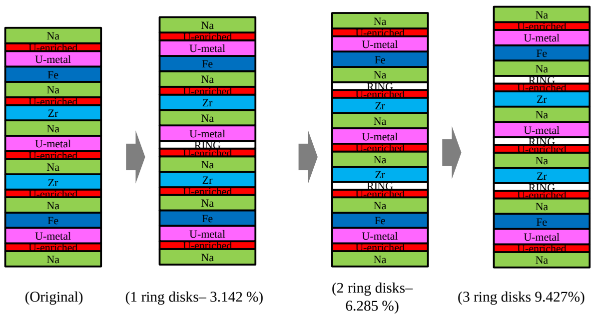

Fig. 7. Axial expansion models in the outer core

3. Analysis Results for Axial Expansion Models

In this study, the MCNP5 code [10] was used with continuous energy ENDF/B-VII.0 library. 200,000 histories per generation, 50 inactive generations, and 300 active generations were used for MCNP5 calculation.

Neutron spectra of the experimental model and the target core are shown in Fig. 8. Two spectra were in good agreement above the 2 keV energy range. Although the experimental model showed a softened spectrum below the 2 keV energy range due to the effect of the temperature difference, neutrons at that energy range were not a significant portion of the total neutrons: 0.7 % in the experimental model and 0.3 % in the target core.

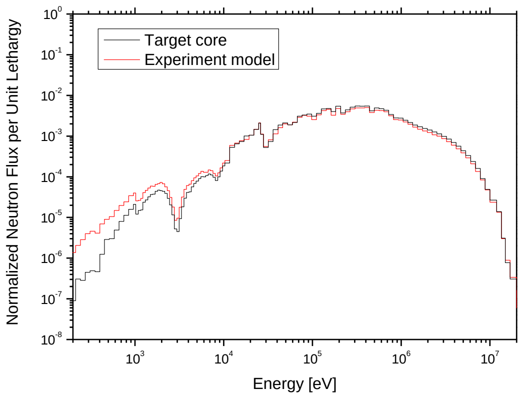

Fig. 8. Neutron spectrum at core central region

Figs. 9 and 10 showed axial expansion reactivities in both the experimental model and the target core. Due to differences in enrichment, the experimental model showed higher axial expansion reactivities at the inner core and lower axial expansion reactivities at the outer core. However, the slopes of the axial expansion reactivities in both the inner and outer cores of the experimental model were similar to those of the target core.

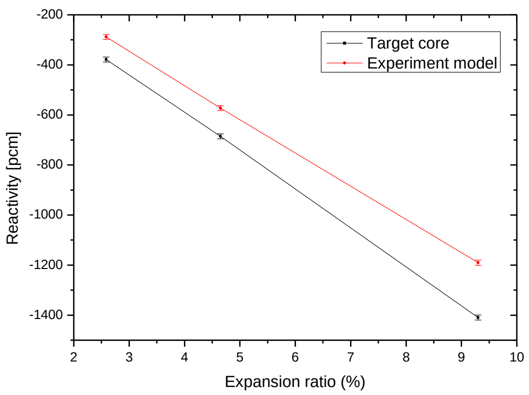

Fig. 9. Axial expansion reactivities of inner core

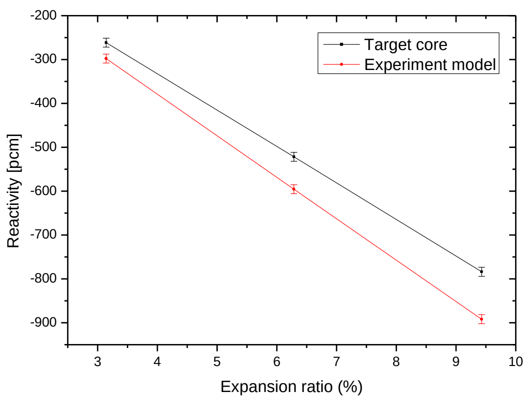

Fig. 10. Axial expansion reactivities of outer core

Table I showed axial expansion reactivity coefficients ($hd\rho/dh$). These coefficients were calculated from the results in Figs. 9 and 10. Reactivity coefficients of the experimental model showed a similar trend as the axial expansion reactivities; the experimental model showed underestimated reactivity coefficients in inner core, and overestimated reactivity coefficients in outer core. However, the whole core reactivity coefficients of the experimental model showed good agreement with those of the target core.

Table I. Reactivity Coefficients ($hd\rho/dh$) for Axial Fuel Expansion

	Inner core	Outer core	Whole core
Target core pcm/%	-152.6±8.1	-83.1±8.3	-235.7±11.6
Experiment model pcm/%	-135.0±8.1	-94.5±8.3	-229.5±11.6
Difference of mean %	-11.5	13.7	-2.6

4. Conclusions and Further Studies

To validate the axial expansion reactivity coefficients of the PGSFR core, experimental models were established based on the BFS critical facility. Three expansion models were developed for each core region. Although the reactivity coefficients of the experimental models in the inner and outer core region showed 11 ~ 14 % differences compared to the target core, the reactivity coefficients in the whole core region showed good agreement. In other words, the proposed experimental model can reflect the axial expansion phenomenon of the target core well.

The axial expansion reactivities will be measured in the Russian BFS facility using the proposed model during 2015. After measurement, an evaluation of the uncertainty and bias for the axial expansion reactivity coefficient is planned as future work.

Acknowledgements

This work was supported by the National Research Foundation of Korea (NRF) grant funded by the Korea government (MSIP). (No. NRF-2012M2A8A2025622)

References

1. Joo HK, et. al., “Status of the Fast Reactor Technology Development in Korea,” *the 48th TWG-FR Meeting*, Obninsk, Russia, May 25-29 (2015).
2. Chang YI, “Technical rationale for metal fuel in fast reactors,” *Nuclear Engineering and Technology*, **39**, 161 (2007).
3. Harish R, Srinivasan GS, Riyas A, and Mohanakrishnan P, “A comparative study of

unprotected loss of flow accidents in 500 MWe FBR metal cores with PFBR oxide core," *Annals of Nuclear Energy*, **36**, 1003 (2009).
4. Planchon HP, Golden GH, Sackett JI, Mohr D, Chang LK, Feldman EE, and Betten PR, "Results and Implications of the Experimental Breeder Reactor II Inherent Safety Demonstration Tests," *Nuclear Science and Engineering*, **100**, 549 (1988).
5. Sathiyasheela T, Riyas A, Sukanya R, Mohanakrishnan P, and Chetal SC, "Inherent safety aspects of metal fuelled FBR," *Nuclear Engineering and Design*, **265**, 1149 (2013).
6. Yun S and Kim SJ, "Comparison of Fuel Axial Expansion Characteristics between the BFS-109-2A Experiment Model and the Target Uranium Core Model," *Transactions of the Korean Nuclear Society Spring Meeting*, May 29-30, Jeju, Korean Nuclear Society(2014) (CD-ROM).
7. Yun S and Kim SJ, "Similarity Assessment of the BFS-109-2A Axial Expansion Experiment Using a Novel Jacobian Matrix Method," *Transactions of the American Nuclear Society*, **111**, 1290 (2014).
8. Yun S, "Experiment Plan for the Uranium Core Mock-up Physics Experiment", KAERI/TR-5648/2014, KAERI (2014).
9. Klinov DA, et. al., "Final Report : Results of Experimental Research of Neutronic Characteristics on the Critical Assembly – SFR Reactor Model," IPPE (2013).
10. X-5 Monte Carlo Team, *MCNP A General Monte Carlo N-Particle Transport Code, Version 5*, Los Alamos National Laboratory (2003).